PARTICLE MIGRATION OF QUASI-STEADY FLOW IN CONCENTRATED SUSPENSION FOR POWDER INJECTION MOLDING

X. Chen, Y. C. Lam, K.C. Tam and S.C.M. Yu

Abstract-**A hybrid FEM/FDM algorithm for particle migration of quasi-steady flow in concentrated suspension materials is proposed in this study. This hybrid FEM/FDM algorithm in which the planar variables, such as pressure field, are described in terms of finite element method, and gapwise variables of temperature, density concentration and time derivatives are expressed by finite difference method. The particle concentration inhomogeneities can be predicted, which is ignored by the existing injection molding simulation packages. Simulation results indicated that powder concentration variation could be significant in practical processing in PIM.**

1. INTRODUCTION

Powder injection molding (PIM) is an important net-shape manufacturing process. It can produce complex shaped, high performance and low cost metallic or ceramic components, with relatively greater design flexibility than conventional powder metallurgy and viable for all shapes that can be formed by injection molding techniques.

Numerical analysis of injection molding filling process of conventional thermoplastic is relatively successful [1- 2]. Some researchers [3- 4] applied the same numerical simulation techniques developed for thermoplastic for the analysis of the PIM filling process with no consideration of the peculiarity of the PIM manufacturing processes, in particular particle migration, which has an effect on the mold-filling behavior. Iwai et al [5], using an alternative approach namely granular mechanics method, predict the motion of individual particles during mold-filling. The kinematical change of powder density is taken into consideration with an explicit evaluation of particle-binder interaction and powder characteristics, such as particle size and distribution.

X. Chen is with the Innovation in Manufacturing Systems and Technology (IMST) Singapore-MIT Alliance, N2-B2C-15, Nanyang Technological University, Nanyang Avenue, Singapore 639798, Phone: (65) 7904273, Fax: (65) 8627215, Email: mxchen@ntu.edu.sg

Y.C. Lam is with the Innovation in Manufacturing Systems and Technology (IMST) Singapore-MIT Alliance, N2-B2C-15, Nanyang Technological University, Nanyang Avenue, Singapore 639798, Phone: (65) 7905866, Fax: (65) 8627215, Email: myclam@ntu.edu.sg

K.C.Tam is with the Molecular Engineering of Biological And Chemical Systems (MEBCS) Singapore-MIT Alliance, N2-B2C-15, Nanyang Technological University, Nanyang Avenue, Singapore 639798, Phone: (65) 7905590 Fax: (65) 8627215, Email: mkctam@ntu.edu.sg

S.C.M.Yu is with School of Mechanical & Production Engineering, Nanyang Technological University, Nanyang Avenue, Singapore 639798

However, such an approach limits the number of particles that can be considered before the computational effort becomes excessive. Thus, its potential for simulating industrial process is limited.

Various investigators had proposed shear-induced particle migration theory to explain a number of flow phenomena for concentrated suspensions including particle accumulation and a blunted velocity profile in simple flow systems. Leighton and Acrivos [6-7] suggested phenomenological models for particle migration in inhomogeneous shear flow. Using Stokesian Dynamics, Nott and Brady [8] have recently carried out dynamic simulations of pressure-driven flow for a suspension in a two-dimensional channel with respect to a monolayer of identical spherical non-Brownian particles. Their simulations confirmed the Leighton and Acrivos shear induced migration theory. Philipes et al [9] adapted the scaling arguments of Leighton & Acrivos, together with an empirical relationship between the suspension viscosity and particle concentration, to predict particle migration for inhomogeneous shear flows. As reported by Karnis et al [10], the velocity profile of a flowing suspension in a circular channel was blunt, compared to the typical parabolic profile. Averbakh et al [11] and Koh et al [12] described an experimental method of measuring velocities in slow viscous flows of highly concentrated suspensions with Laser Doppler Anemometry technique. Their measurements confirmed that velocity profiles in a concentrated suspension were blunt due to the migration of particles from high shear area to low shear area and it was different from those for a Newtonian fluid. However, these phenomenon have never been considered by the PIM community.

In this investigation, a new numerical approach which has the potential of general applicability, but targeting the simulation of practical powder injection molding process, is proposed. The present analytical and numerical development can provide an insight into the mold filling process so as to predict the concentration distribution of the powder, a major characteristic of powder injection molding. The proposed model is based on the generalized Hele-Shaw flow model[13] for thin cavities, coupled with a diffusion model which describes the interaction between powder and binder. The rheological behavior of the feedstock was evaluated using a Krieger model [14] to account for the viscosity dependency on shear rate and powder concentration. The simulated results indicated that powder concentration variation could be significant and most of the key parameters for filling process would change due to a change in powder concentration distribution.

2. MATHEMATICAL MODEL

a) Governing equations

The Hele-Shaw type flow model provides a reasonably accurate description of polymer flow in thin cavities. For our preliminary investigation of PIM for thin cavity, we adopt a similar approach. Thus, the resultant sets of conservative equation can be written as:

$$\frac{\partial(b\overline{u})}{\partial x} + \frac{\partial(b\overline{v})}{\partial y} = 0 \tag{1}$$

$$\frac{\partial P}{\partial x} = \frac{\partial}{\partial z}(\eta \frac{\partial u}{\partial z}), \quad \frac{\partial P}{\partial y} = \frac{\partial}{\partial z}(\eta \frac{\partial v}{\partial z}) \tag{2}$$

$$\rho C_v(\frac{\partial T}{\partial t} + u\frac{\partial T}{\partial x} + v\frac{\partial T}{\partial y})$$

$$= K\frac{\partial^2 T}{\partial z^2} + \eta[(\frac{\partial u}{\partial z})^2 + (\frac{\partial v}{\partial z})^2] \tag{3}$$

where the continuity equation is expressed in terms of gapwise averaged velocity components $\overline{u}$ and $\overline{v}$, with u and v the velocity components in the x and y directions respectively. b is the half thickness, η the shear viscosity and P the cavity pressure. In the energy equation, ρ is the feedstock effective density, C_v the effective specific heat, and K the effective thermal conductivity. When the no slip boundary condition is employed at the wall, the following pressure equation derived from the momentum and continuity equations can be obtained:

$$\frac{\partial}{\partial x}(S\frac{\partial P}{\partial x}) + \frac{\partial}{\partial y}(S\frac{\partial P}{\partial y}) = 0 \tag{4}$$

where

$$S = \int_0^b \frac{z^2}{\eta}dz \tag{5}$$

which S is the flow conductance.

When a suspension (powder/binder mixture) is subjected to inhomogeneous shear flow in the cavity, shear-induced diffusion of particles takes place. Following the diffusive flux model of Phillips et al [9], the implementation of the diffusion equation can be written as[15]:

$$\frac{\partial\phi}{\partial t} + \frac{\partial(u\phi)}{\partial x} + \frac{\partial(v\phi)}{\partial y}$$

$$= a^2\{\frac{\partial}{\partial z}[\dot{\gamma}\phi(K_c + K_\eta\phi\frac{1}{\eta}\frac{\partial\eta}{\partial\phi})\frac{\partial\phi}{\partial z}] + \frac{\partial}{\partial z}(K_c\phi^2\frac{\partial\dot{\gamma}}{\partial z}]\} \tag{6}$$

where ϕ is particle concentration by volume, a is the characteristic particle radius, $\dot{\gamma}$ is the local shear rate, K_c and K_η are the empirically determined diffusion coefficients.

b) Boundary conditions

The pressure equation (4) is a differential equation of elliptic type and thus requires the boundary conditions to be specified along all boundaries. At the moving front, it is assumed that the pressure is constant. For the sake of simplicity, this constant is set to zero:

$$P\big|_{front} = 0. \tag{7}$$

At the gate, the flow rate is usually specified as a function of time. This condition can be stated as:

$$2\oint_{gate}(S\frac{\partial P}{\partial n})ds = Q \tag{8}$$

where n is the outward normal to the boundary and Q is flow rate across the entire gap. On the cavity wall, it is required that the normal component of the velocity vanish as:

$$\partial P/\partial n = 0 \tag{9}$$

Since the conduction in the x and y directions is neglected in the energy equation, only the temperature on the walls of the mold has to be given:

$$T\big|_{wall} = T_w \tag{10}$$

At the gate the temperature is assumed to be uniform and equal to the melt temperature. At the flow front, the fountain flow carried the material from the core and deposits it on the cavity wall. A scheme has been developed [16] to account for the effect of the fountain flow on the temperature field. In our investigation, the temperature at the flow front is taken as the temperature in the core of the cavity.

Diffusive-flux equation (6) also must be supplemented with appropriate boundary conditions at the wall, which is subjected to the usual no slip condition, $\mathbf{u} = 0$, and no particle flux expressed as:

$$\{\dot{\gamma}\phi(K_c + K_\eta\phi\frac{1}{\eta}\frac{\partial\eta}{\partial\phi})\frac{\partial\phi}{\partial z} + K_c\phi^2\frac{\partial\dot{\gamma}}{\partial z}\}\cdot\mathbf{n} = 0 \tag{11}$$

where $\mathbf{n}$ is the outward normal unit vector. The particle concentration ϕ is assumed to be uniform initially at the entrance or the gate and expressed as:

$$\phi = \phi_0 \text{, for } -b \le z \le b. \tag{12}$$

c) Material models

The viscosity of the bulk material is taken to be a function of the neat binder viscosity and the volume fraction of the powder. We have adopted the Krieger rheological model [14].

$$\eta = \eta_b (1 - \frac{\phi}{\phi_c})^{-m} \tag{13}$$

where η_b is the viscosity of binder. m is material constant. ϕ and ϕ_c are the powder concentration and the critical powder loading respectively. This rheological model describes the effect of the volume fraction of the powder on the flow behaviour of powder/binder mixture. The viscosity relationship for the binder is approximated using the following power law viscosity model:

$$\eta_b = g(T)\dot{\gamma}^{n-1} , \ \dot{\gamma} = \sqrt{(\partial u/\partial z)^2 + (\partial v/\partial z)^2} \tag{14a}$$

$$g(T) = m_0 \exp(T_a/T) \tag{14b}$$

where n, m_0 and T_a are material constants. As the powder distribution ϕ is calculated, the feedstock effective density ρ and specific heat C_v can be determined respectively using the linear rule of mixture as follows:

$$\rho = \rho_1 \phi + \rho_2 (1 - \phi) \tag{15}$$

$$C_v = C_{v1} \phi + C_{v2} (1 - \phi) \tag{16}$$

where ρ_1 and ρ_2 are density of the binder system and powder particle respectively. C_{v1} and C_{v2} are the specific heat of the binder system and powder particle respectively.

To estimate the effective thermal conductivity K, Jeffrey's equation is adopted, which should give a better approximation than the linear rule of mixture. Jeffrey's equation can be represented as[17]:

$$K = \left\{ 1 + 3\zeta\phi + \phi^2 (3\zeta^2 + \frac{3\zeta^3}{4} \right.$$

$$\left. + \frac{9\zeta^3}{16} \frac{\lambda+2}{2\lambda+3} + \frac{3\zeta^4}{64}) \right\} \cdot K_m \tag{17}$$

where $\lambda = K_f/K_m$ and $\zeta = (\lambda - 1)/(\lambda + 2)$, K, K_f and K_m are the thermal conductivity of feedstock, particles and binder matrix respectively. ϕ is the particle volume fraction.

3. NUMERICAL IMPLEMENTATION

a) The pressure equation

Galerkin's method can be applied to the pressure equation, equation (4) as a finite element formulation, which can be described as follows:

$$\iint_\pi [\frac{\partial}{\partial x}(S\frac{\partial P}{\partial x}) + \frac{\partial}{\partial y}(S\frac{\partial P}{\partial y})] \cdot W_i d\pi = 0 \tag{18}$$

with the weighting function W_i being zero where pressure boundary condition is imposed. Integration by parts and applying the divergence theorem, one obtains

$$\oint_{\partial\pi} [(S\frac{\partial P}{\partial x})\cdot n_x + (S\frac{\partial P}{\partial y})\cdot n_y] \cdot W_i ds$$

$$- \iint_\pi [(S\frac{\partial P}{\partial x})\cdot\frac{\partial W_i}{\partial x} + (S\frac{\partial P}{\partial y})\cdot\frac{\partial W_i}{\partial y}] d\pi = 0 \tag{19}$$

where n_x and n_y are the components of outward unit normal vector on the boundary. Since W_i is zero where pressure condition is imposed,

$$(S\frac{\partial P}{\partial x})\cdot n_x + (S\frac{\partial P}{\partial y})\cdot n_y = 0 \tag{20}$$

Along the cavity wall boundary due to the impermeable condition, the first integral term vanish in equation (19). Therefore, equation (19) can now be rewritten as

$$\iint_\pi [(S\frac{\partial P}{\partial x})\cdot\frac{\partial W_i}{\partial x} + (S\frac{\partial P}{\partial y})\cdot\frac{\partial W_i}{\partial y}] d\pi = 0 \tag{21}$$

which is a weak form statement of equation (4) incorporating boundary conditions. With the finite element discretization of the domain π, Equation (21) can be rewritten as a summation over the elements as follows:

$$\sum_e \iint_{\pi_e} [(S\frac{\partial P}{\partial x})\cdot\frac{\partial W_i}{\partial x} + (S\frac{\partial P}{\partial y})\cdot\frac{\partial W_i}{\partial y}] d\pi = 0 \tag{22}$$

Approximate pressure P over each element can be interpolated by shape functions N_i and nodal pressure p_i ($i = 1,2,3$):

$$P = N_1 p_1 + N_2 p_2 + N_3 p_3 \tag{23}$$

Introducing equation (23) into equation (22) and letting $W_i = N_i$ gives

$$\sum_e K_{ij}^e p_j^e = 0 \tag{24}$$

where

$$K_{ij}^e = \iint_{\pi_e} (S\frac{\partial N_i}{\partial x} \cdot \frac{\partial N_j}{\partial x} + S\frac{\partial N_i}{\partial y} \cdot \frac{\partial N_j}{\partial y})d\pi \tag{25}$$

Equation (24) can be restated in the form of a global matrix equation:

$$[\overline{K}]\{\overline{P}\} = \{\overline{C}\} \tag{26}$$

where $[\overline{K}]$ is the stiffness matrix for the system, $\{\overline{P}\}$ denotes the vector of unknown pressures and $\{\overline{C}\}$ denotes the forcing vector depending on the given flow rate and the pressure boundary conditions. Equation (26) is a nonlinear system of equations for pressure field and thus requires an iteration procedure to obtain a convergent numerical solution. Estimates of $P(x, y)$ can be obtained by solving equation (26) with an initial value of S. Subsequently, S, which is function of the viscosity η, is updated using equation (5). A new $[\overline{K}]$ is then obtained. A more accurate $P(x, y)$ can be estimated by solving equation (26) again. This iteration procedure is repeated under a converged solution is obtained.

b) The energy equation

The energy equation (3) is discretized using finite difference method. The time derivative of temperature is approximated by the backward difference scheme:

$$\frac{\partial T}{\partial t} = \frac{1}{\Delta t}(T_z^t - T_z^{t-\Delta t}) \tag{27}$$

and the z-derivative by the central difference scheme:

$$\frac{\partial}{\partial z}(K\frac{\partial T}{\partial z}) = \frac{1}{\Delta z^2}([KT]_{z+\Delta z}^t - 2[KT]_z^t + [KT]_{z-\Delta z}^t) \tag{28}$$

The viscous dissipation term and the convection term are evaluated using the solution from the previous time step. This method allows the calculation of the temperature as a function of time and thickness position from node to node.

c) The diffusive-flux equation

The equation (6) can be written in the following conservative finite difference form:

$$\frac{\phi_{i,z}^t - \phi_{i,z}^{t-\Delta t}}{\Delta t} + \sum_{k=1}^3 \frac{\partial N_k}{\partial x}(u\phi)_{k,z}^{t-\Delta t} + \sum_{k=1}^3 \frac{\partial N_k}{\partial y}(v\phi)_{k,z}^{t-\Delta t}$$

$$= \frac{(\hat{D}_{i,z+\Delta z}^{t-\Delta t} + \hat{D}_{i,z}^{t-\Delta t})\phi_{i,z+\Delta z}^t + (\hat{D}_{i,z-\Delta z}^{t-\Delta t} + \hat{D}_{i,z}^{t-\Delta t})\phi_{i,z-\Delta z}^t}{2\Delta z^2}$$

$$- \frac{(\hat{D}_{i,z+\Delta z}^{t-\Delta t} + 2\hat{D}_{i,z}^{t-\Delta t} + \hat{D}_{i,z-\Delta z}^{t-\Delta t})\phi_{i,z}^t}{2\Delta z^2}$$

$$+ \frac{(\tilde{D}_{i,z+\Delta z}^{t-\Delta t} + \tilde{D}_{i,z}^{t-\Delta t})\dot{\gamma}_{i,z+\Delta z}^t + (\tilde{D}_{i,z-\Delta z}^{t-\Delta t} + \tilde{D}_{i,z}^{t-\Delta t})\dot{\gamma}_{i,z-\Delta z}^t}{2\Delta z^2}$$

$$- \frac{(\tilde{D}_{i,z+\Delta z}^{t-\Delta t} + 2\tilde{D}_{i,z}^{t-\Delta t} + \tilde{D}_{i,z-\Delta z}^{t-\Delta t})\dot{\gamma}_{i,z}^t}{2\Delta z^2} \tag{29}$$

where

$$\hat{D}_{i,l}^{t-\Delta t} = \dot{\gamma}_{i,l}^{t-\Delta t}\phi_{i,l}^{t-\Delta t}a^2(K_c + \frac{K_\eta \phi_{i,l}^{t-\Delta t}m}{\phi_c - \phi_{i,l}^{t-\Delta t}}),$$

$$(l = z + \Delta z, z, z - \Delta z) \tag{30}$$

$$\tilde{D}_{i,l}^{t-\Delta t} = (\phi_{i,l}^{t-\Delta t})^2 a^2 K_c,$$

$$(l = z + \Delta z, z, z - \Delta z) \tag{31}$$

The diffusive-flux equation (6) is solved by an implicit conservative finite difference scheme in the gapwise direction with particle concentration evaluated at the node of each element. The convection particle flux and shear-induced particle flux are evaluated using the particle concentration from the previous time step, while a backward difference method is used for transient and particle concentration gradient flux terms. This results in a symmetric tri-diagonal matrix which can be solved using Gauss-Seidel method after solving the particle concentration at the wall from equation (11).

4. NUMERICAL RESULTS AND DISCUSSION

The rheological data of binder system employed for the numerical examples are $m_0 = 2.824 \times 10^{-4} Pa \cdot s^n$, $T_a = 2138K$ and $n = 0.99$. The density of iron powder and binder are $\rho_1 = 7.87 g/cm^3$ and $\rho_2 = 0.91 g/cm^3$ respectively. The specific heat capacity of iron powder and binder are $C_{v1} = 328.3 J/kg \cdot K$ and $C_{v2} = 2790 J/kg \cdot K$ respectively. The thermal conductivity of iron powder and binder are $K_f = 75.8W/m \cdot K$ and $K_m = 0.024W/m \cdot K$ respectively. Employing the Krieger model of suspension, we assume that $m = 1.82$.

a. A box cavity

A box cavity has been chosen to demonstrate the effects of powder density distribution on flow and heat transfer during the mold filling stage. The dimensions of the box are 30cm by 10cm by 20cm with a thickness of 0.2cm. The finite element mesh is shown in Figure 1 (766 elements, 444 nodes). Node G
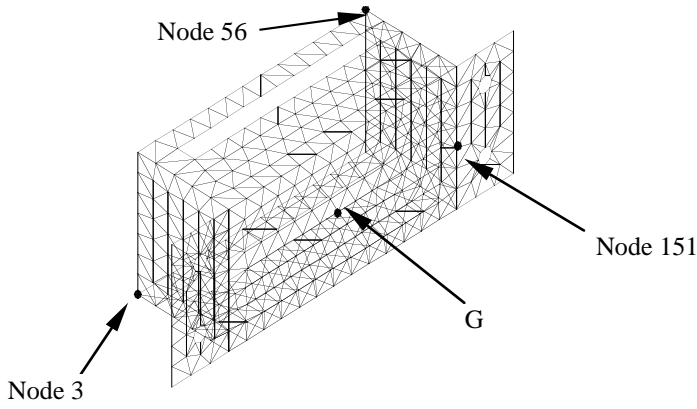
Figure 1 Mesh of the box cavity.

the gate location. The molten feedstock temperature is $240\,^{o}C$, filling time is 5s. The mold temperature is $80\,^{o}C$.

To investigate the effects of powder density on the filling stage, powder concentration distribution and effective viscosity were assumed to be uniform at the gate. Non-isothermal simulations with the assumption of with and without particle migration were carried out. Without particle migration, uniform particle density distribution would always be predicted, which is not realistic. With particle migration, a final inhomogenous green part would be predicted.

b) Effect of the mesh size

In order to evaluate the sensitivity of the results with mesh size, three mesh sizes have been tested: (i) 346 elements , (ii) 766 elements as shown in Figure 3 and (iii) 940 elements. Computational time about 101s, 212s, and 253s on a PC586 Pentinum III(RAM 284Mb) for cases (i), (ii) and (iii) respectively.

The evolution of pressure versus filling time at the gate has been plotted for the three cases in Figure 2. The pressure at the gate was slightly higher for the coarse mesh cases (i) but there was little difference between cases (ii) and (iii). Thus, for all subsequent calculation, a mesh size of 766 elements was employed.
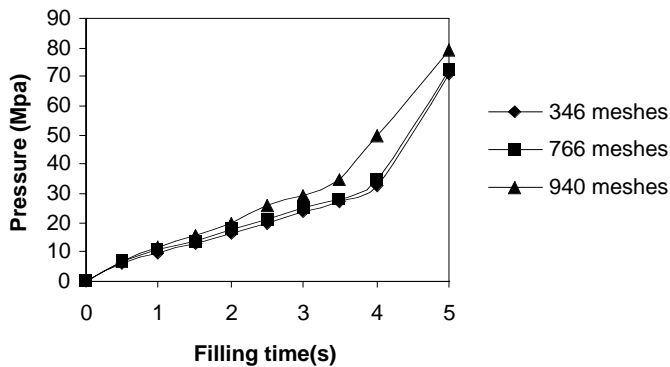

Figure 2 Gate pressure evolution for three mesh sizes

c. *Effect of diffusion constant K_c and K_η*

There are no experimental data on the diffusion coefficients for iron powder mixtures. Thus, the diffusion constants K_c and K_η were chosen respectively to be 0.and 0., 0.43 and 0.65, 0.55 and 0.65 in order to observe the effect of the diffusion constant on particle migration. In addition, mono-size iron powder particles of $50\,\mu m$ in radius were assumed for each simulation. As expected, from shear-induced diffusion model, equation (11), powder migrated toward these low shear regions from high shear regions resulting in powder accumulation as shown in Figure 3(a). For $K_c/K_\eta = 0.66$ (K_c =0.43 and K_η =0.65) and initial concentration $\overline{\phi} = 45\%$, the maximum bulk powder concentration is approximately 46.5%. The minimum bulk powder concentration is approximately 43.5%. Figure 3(b)
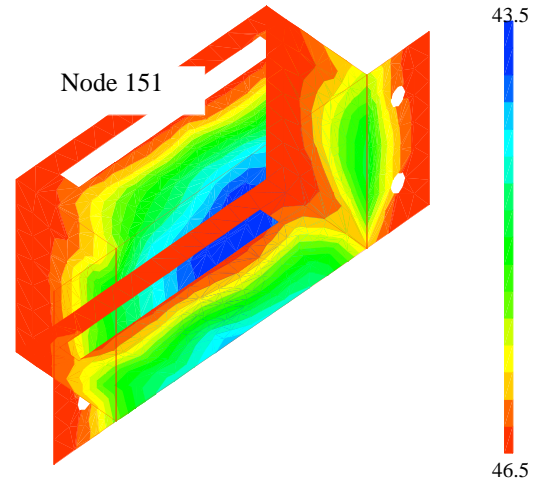

Figure 3(a) Predicted bulk powder concentration(%) distribution with K_c/K_η =0.66 and $\overline{\phi} = 45\%$
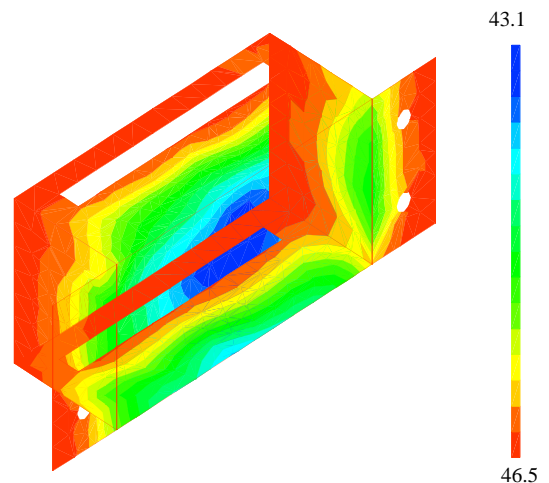

Figure 3(b) Predicted bulk powder concentration(%) distribution with K_c/K_η =0.90 and $\overline{\phi} = 45\%$

shows the through thickness average (bulk) distribution powder concentration of the part with $K_c/K_\eta = 0.90$ (K_c =0.55 and K_η =0.65) at the end of filling with the same initial concentration as in Figure 3(a). The maximum bulk powder concentration is approximately 47.8%. The minimum as in bulk powder concentration is approximately 43.1%. As expected, with larger K_c/K_η , there was greater particle density variation.

d. Through thickness powder concentration and velocity distribution

To further illustrate the effect of particle migration on velocity profiles and particle density distribution, the
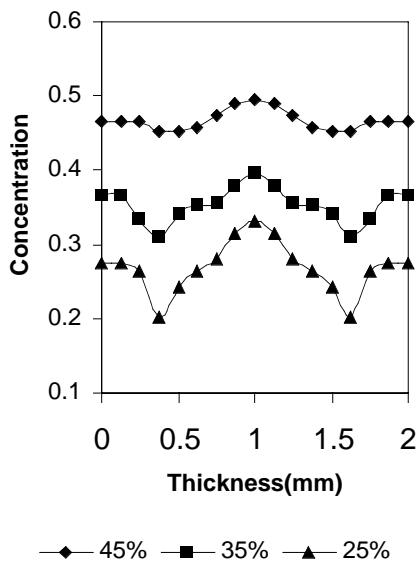

Figure 5 Through thickness velocity profiles at end of filling (t=5s) at node 151 in Figure 1

The migration of particles to the midplane resulted in an increase in effective viscosity. This in turns blunted the velocity profiles at the midplane. This prediction is in agreement with the computational results of Brady [8] who employed Stokesian Dynamics method for viscous flows of concentrated suspensions exhibiting shear-induced particles migration.

5. CONCLUSIONS

In this investigation, a numerical model based on a FEM/FDM hybrid method has been developed to simulate the powder injection molding process with particle migration. Powder distribution can be predicted through the introduction of diffusion equation at the nodal control volume level. The model can predict the variation of powder density distribution which is ignored by the existing simulation packages. Particle migration reduced the pressure required for the process as viscous dissipation of energy was reduced. Preliminary simulation indicated that powder concentration variation could be significant. Non-isothermal analysis indicated that most of the key parameters for filling process would change due to a change in powder concentration distribution. These numerical results elucidated the importance of particle migration for non-isothermal flow.

Figure 4 Through thickness concentration profiles at end of filling(t=5s) at node 151 in Figure 1

initial concentration was chosen to be $\bar{\phi} = 0.\%$, 25%, 35% or 45%. Figure 4 shows powder concentration profiles at node 151 for different initial concentrations. It is evident that powder concentration at the midplane increased considerably with a corresponding significant decrease in powder concentration near the wall. This was caused by the relatively high shear rate near the wall and negligible shear rate at the midplane of the part. As the resulting effective viscosity along the thickness direction was highly non-uniform, it increased considerably at the stagnation area such as the corner (node 56 and node 3 in Figure1). This would result in high powder concentration as illustrated in Figure 3a) and 3b).

The changes in the through thickness direction for concentration and effective viscosity were further reflected in the velocity profiles as shown in Figure 5.
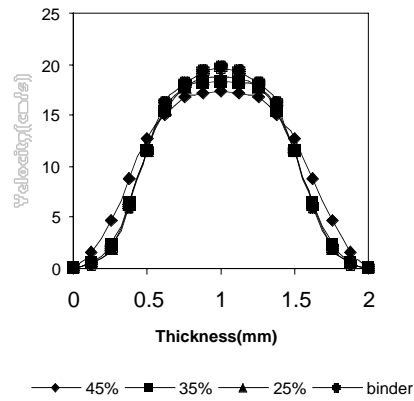
REFERENCES

1. Randall M. German, Powder Injection Molding, Metal Powder Industries Federation,*Princeton*, N.J,(1991).
2. Hens K.F. and Lee D., Process Analysis of Injection Molding with Powder Products, *Advances in Powder Metallurgy*,MPIF,APMI, **2**, 127, (1991).
3. Najami L.A and Lee D, Application of Mold Filling Simulation to Powder Injection Molding, *Polym. Eng. Sci*,**30**,231,(1994).
4. Kwon T.H and Park J.B, Finite Element Analysis Modelling of Powder Injection Molding Filling Process Including Yield Stress and Slip Phenomena, *Polym.Eng. Sci.*,**35**,741,(1995).
5. Iwai T., Aizawa T. and Kihara J., Powder-Binder Flow Simulation in Powder Injection Molding, *Proc.Powder Injection Molding Symp.*,MPIF, (1996).

6. Leighton D. and Acrivos A., The shear-induced self-diffusion in concentrated suspensions. *J. Fluid Mech*. **181**,415, (1987a).

7. Leighton D. and Acrivos A., Measurement of shear-induced self-diffusion in concentrated suspensions of spheres. *J. Fluid Mech*. **177**,109, (1987b),

8. Nott P. R. and Brady J.F., Pressure-driven flow of suspensions:simulation and theory, *J. Fluid Mech*. , **275**,157, (1994).

9. Phillips R.J, Armstrong R. C., Brown R.A., A Graham A.L. and Abbott J.R., A constitutive model for concentrated suspensions that accounts for shear-induced particle migration*, Phys. Fluids A* ,**4**,31, (1992).

10. Karnis A., Goldsmith H.L., and Mason S.G., "The kinetic of flowing dispersions:I Concentrated Suspensions of Rigid Particles",*J.Colloid Interface Sci*.**22,**531, (1996).

11. Averbakh A., Shauly A., Nir A. and Semiat R. , Slow viscous flows of highly concentrated suspensions-parts I: Laser-Doppler Velocimetry in rectangular ducts, int. *J. Multiphase flow,* **23**, 409, (1997).

12. Koh C., Leal J.L.G and Hookham P.A.,"An Experiment Investigation of Concentrated Suspension Flow in a Rectangular Channel", *J Fluid Mech*. **256**,1, (1994).

13. Hieber C.A. and Shen S.F., A Finite-Element /Finite-Difference Simulation of the Injection-Molding Filling Process, *J.Non-Newton Fluid Mechanics*, **7**,1, (1980)

14. Kriger I. M., Rheology of monodisperse lattices. *Adv. Colloid Interface Sci.,* **3**, 111, (1970).

15. Y.C. Lam, X. Chen, K.C. Tam and S.C.M. Yu, Computation Fluid Dynamics Simulation of Powder Injection Molding, *PIM2000-International Conference on Powder Injection Molding of Metals and Ceramics*, USA, March 20-22,2000.

16. Dupret F. and Vanderschuren L., Calculation of the Temperature Field in Injection Molding, *AICHE J.*, **34**,1959,(1988)

17. Rhee B.O, Processing Behaviour of Powder /Binder Mixtures in Powder Injection Molding-Binder Separation and Quick Freezing, *PhD dissertation*,(1992).